IRON-RICH NONFERROUS-METALLURGY SLAGS IN CERAMICS

A. A. Plashchenko and M. Yu. Chop

UDC 669.054.8:691.4

Some facing materials are improved considerably by the use of slags from ferrous metallurgy, chemical or other engineering processes, and thermal power stations. However, little attention has been given to slags from nonferrous metallurgy in making ceramic sheet materials; hardly any use has been made of them. These slags may contain up to 35%* or more iron oxides, mainly ferrous oxide.

In the literature, on the one hand, it has been shown that it is undesirable for there to be large amounts of iron in raw materials on account of the staining action [1], while on the other, it has been found that ferrous oxide has a considerable fluxing effect in ceramic sintering [2]. However, the precise mechanisms in the latter have not been established for iron-rich slags. Also, the imminent exhaustion of high-grade traditional raw material will very soon make it inevitable that low-grade material will be used, including iron-rich slags. Such additives provide for bulk coloring in ceramic facings, which might reduce the consumption of expensive ceramic pigments.

We have therefore examined a representative group of iron-rich nonferrous-metallurgy slags in order to extend ceramic raw materials, reduce the adverse effects from wastes, and improve industrial economy.

We examined three types of cobalt-nickel slag from the Bug nickel plant: medium-iron acid (SZh), high-iron basic (VHz), and low-iron acid (MZh), as well as two slags in the tin-lead group from the Ukrtsink plant: OS1 and OS2. We chose several slags of the same type in order to elucidate the effects from various mineral and chemical components and from inhomogenei-

TABLE 1

Material	Mass contents, %													
	SiO_2	Al_2O_3	TiO_2	FeO	Fe_2O_3	CaO	MgO	Na_2O	K_2O	SO_3	organic components	ignition loss	NiO+MnO+ +CoO+Cr_2O_3	ZnO+PbO
SZh	36,71	3,86	0,34	33,91	7,14	8,51	4,08	0,33	0,06	0,19	—	—	4,97	—
VZh	18,47	2,05	0,60	25,58	28,43	17,35	2,04	0,27	0,06	0,29	—	—	4,86	—
MZh	53,97	4,35	0,37	7,76	1,07	22,41	8,95	0,23	0,19	0,08	—	—	0,62	—
OS 1	23,04	7,37	0,44	21,00	5,40	19,15	10,20	1,81	0,13	4,98	—	—	—	6,48
OS 2	33,10	5,41	0,31	28,60	6,52	20,14	1,83	0,95	0,27	0,34	—	—	—	2,53
Novorai · clay	62,00	23,00	—	—	4,10	0,38	0,52	0,85	1,25	—	0,34	5,90	—	—
DNPK-1														

TABLE 2

Phase	Slag				
	SZh	VZh	MZh	OS1	OS2
SiO_2 — quartz	+	—	+	—	—
$FeO \cdot SiO_2$ — ferrosilite	+	—	+	—	—
$FeO \cdot Fe_2O_3$ — magnetite	+	+	+	—	+
$CaO \cdot FeO \cdot 2SiO_2$ — hedenbergite	—	+	—	—	+
$2CaO \cdot SiO_2$ — belite	—	+	+	—	+
$2CaO \cdot FeO \cdot 2SiO_2$ — akermanite	—	+	—	—	+
$CaO \cdot FeO \cdot SiO_2$ — kirshteinite	—	—	+	+	—
$CaO \cdot MgO \cdot 2SiO_2$ — dioxide	—	—	+	+	—
FeO — wustite	—	—	—	+	—
$2MgO \cdot SiO_2$ — forsterite	—	—	—	+	—
$CaO \cdot MgO \cdot SiO_2$ — monticellite;	—	—	—	—	—
Ratio O : Si	3,2	5,3	2,8	5,0	3,5
Structure pattern	$[(SiO_3)_2]_\infty$	$[SiO_4]$	$[(SiO_3)_2]_\infty$	$[SiO_4]$	$[Si_2O_7]$

*Here and subsequently, mass contents.

Kiev Polytechnical Institute. Translated from Steklo i Keramika, No. 9, pp.2-4, September, 1988.

0361-7610/88/0910-0309$12.50

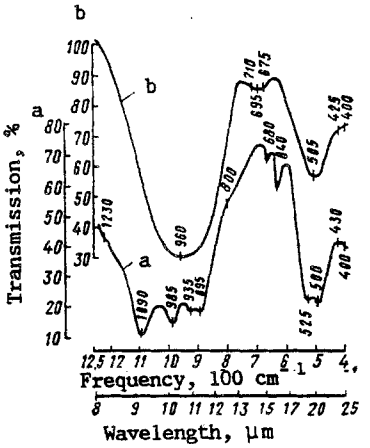

Fig. 1

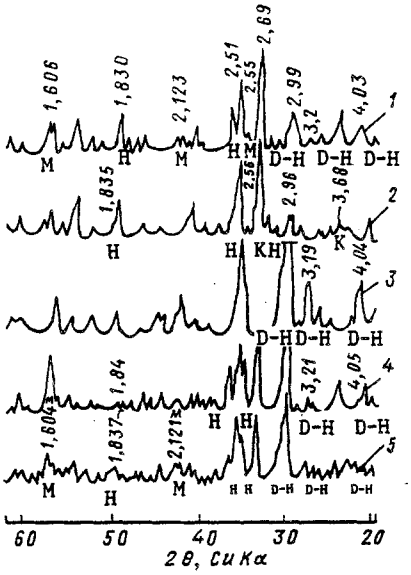

Fig. 2

Fig. 1. IR spectra for initial MZh slag (2a) and OS1 (b).

Fig. 2. X-ray diffraction patterns for slags SZh (1), VZh (2), MZh (3), OS1 (4), and OS2 (5); H) haematite; M) magnetite; K) kirshteinite; D-H) diopside-hedenbergite solid solution.

ties and fluctuations in characteristics on the properties of the ceramics. Such factors are considered as major obstacles to using slags for constructional materials.

Table 1 gives the slag compositions. The main components are: SiO_2, FeO, Fe_2O_3, CaO, MgO, Al_2O_3. We divided the slags into two groups, for which the sum of four of these six oxides constituted 75-90%. For example, the group composed of SZh, VZh, and OS2 had SiO_2 + FeO + Fe_2O_3 + CaO of 90.35; 91.87; 80.19% correspondingly (with allowance for the inclusion of MgO in CaO), while for the group composed of MZh and OS1, SiO_2 + FeO + CaO + MgO was 93.09 and 74.39% correspondingly.

The compositions after conversion to the four corresponding oxides were represented as points within the corresponding tetrahedra [3]. The theoretical phase compositions were determined from these positions (Table 2), and Table 2 also gives the molar O:Si ratios, from which one can represent the various possible combinations of the linked $[SiO_4]^{4-}$ tetrahedra [4].

The IR spectra for the initial MZh and OS1 slags largely confirm the theoretical calculations (Fig. 1). The triply degenerate stretching vibration for $[SiO_4]$ in OS1 lies in the 950 cm^{-1} frequency range and is not seen as separate bands, which indicates that there are symmetrical discrete silicon-oxygen tetrahedra. The Fe^{3+} and Al^{3+} having coordination number 4 (660-730 cm^{-} bands) act as structure formers to an extent much less than Fe^{3+}, Al^{3+}, Fe^{2+}, Mg^{2+} in sixfold coordination (modifies), which is indicated by the deeper bands in the 400-425 cm^{-1} region.

These data show that OS1 is very much vitrified. The 895, 935, 985, 1090 cm^{-1} bands for MZh (Fig. 1a) correspond to asymmetric O–Si–O and Si–O–Si stretching vibrations in the Si_2O_6 unit cell in the pyroxenes. The band at 640 and 680 cm^{-1} correspond to symmetrical Si–O–Si stretching vibrations and also indicate a pyroxene structure. The bands at 525 cm^{-1} correspond to Mg^{2+}–O and Fe^{3+}–O deformation vibrations. That band corresponds to $[MgO_4]$ and $[Fe^{3+}O_4]$ stretching vibrations, while the 410 and 430 cm^{-1} bands correspond to $[MgO_6]$, $[Fe^{2+}O_6]$, and $[Fe^{3+}O_6]$ stretching vibrations. The bands are diffuse, which shows that the MZh contains residual vitreous phase [5].

X-ray diffraction patterns (Fig. 2) serve to identify the phase compositions for slags heated to 1000°C for 2 h. SZh has a predominant set of reflections due to diopside. Magnetite and haematite were also present. In VZh, there were haematite and an insular silicate, kirshteinite. In MZh, the main phase was a pyroxene having a diopside-hedenbergite

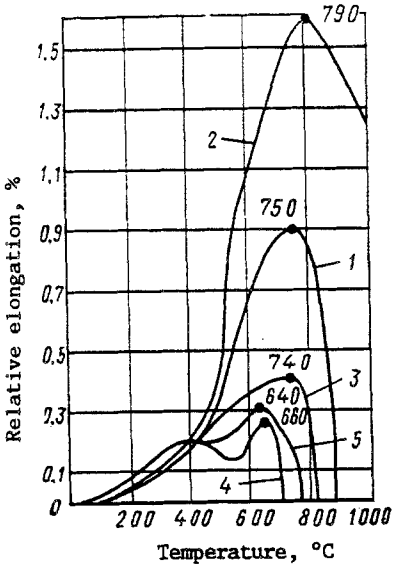

Fig. 3

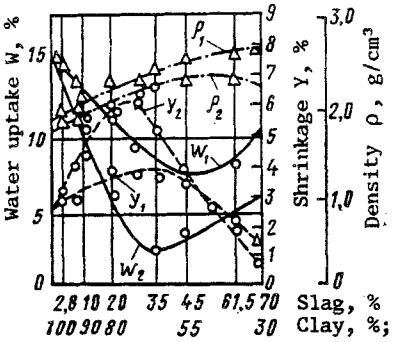

Fig. 4

Fig. 3. Dilation patterns for SZh (1), VZh (2), MZh (3), OS1 (4), and OS2 (5) slags.

Fig. 4. Effects of slags MZh (1) and OS1 (2) on water uptake, shrinkage and density.

composition. The tin-lead slags contained hedenbergite, diopside, quartz, haematite, and magnetite. OS1 also showed pyrrhotite, and OS2 kirshteinite.

The diopside-hedenbergite chains formed by firing can act as reinforcement in the ceramic, in the same way as wollastonite [6]. The minor components and the nonequilibrium production conditions complicated the compositions. Nevertheless, the analysis correctly indicated that pyroxene structure can crystallize here.

A DKV dilatometer was used at 20-900°C to record the thermal expansion (Fig. 3). Earlier softening occurred in the vitreous OS1 and OS2, namely at 660 and 640°C correspondingly. MZh, softened at 740°C, which was due to its greater crystallinity and to polymerization in the silicon-oxygen tetrahedra. The softening temperature for SZh and VZh were the highest: 750 and 790°C.

This suggests that ceramic sintering can be accelerated by adding these nonferrous slags. The clay component was the semiacid Novorai clay, whose composition is given in Table 1. The specimens were prepared by the [7] method. Figure 4 gives the water uptake, shrinkage, and density for specimens containing 0-70% slag after heat treatment at 1000°C for 2 h.

All the slags accelerate the sintering, the sequence as regards this being: OS1 (90% vitreous phase) ≈ OS2 (80%) > MZh (30%) > SZh (8%) ≥ VZh (5%).

These slags differ considerably in chemical and mineral compositions, but the sintering is determined in the main by the vitreous-phase content in the slag (as determined by petrographic methods). The apparent density in the fired material always increased with the slag content, because the high-iron slags had high densities: 3.8-4.5 g/cm³. There were also discrepancies between the maximum shrinkage and minimal water uptake (Fig. 4).

The high productivity in the experiments eliminated effects from random and gross errors (three parallel runs). Slag grains on sintering form a framework that reduces the shrinkage, but in our case this occurred at slag contents not less than 10-15%, while at 0-15% slag, there was an increase in the shrinkage relative to the use of pure clay, which we consider to be due to the slag grains softening when their amounts are small and favoring the structural elements moving one relative to the other. At slag levels over 15-20%, the framework begins to retard the shrinkage.

The sintering tests gave the following % compositions for the optimal materials on a two-component basis: 7P + 28.5 SZh, 10P + 28.5 VZh, 13P + 45.0 MZh, 19P + 28.5 OS1, 25P + 28.5 OS2, balance DNPK-1 clay.

TABLE 3

Parameter*	Mass				
	7P	10P	13P	19P	25P
Water uptake, %	6,7	6,2	6,8	3,8	3,6
Shrinkage, %	5,9	5,3	5,0	6,2	6,2
Apparent density, g/cm³	2,33	2,35	2,32	2,47	2,46
Bending strength, MPa	50,4	52,6	34,8	52,1	49,9

*The frost resistance in all cases was more than 50 cycles.

Experimental batches of ceramic tiles 120 × 65 × 7 mm were made from these materials under industrial conditions. The tiles were pressed at 24 MPa and fired at 1040°C for 50 min in a roller oven (Table 3). These unglazed tiles were dark olive in color (7P and 10P), pale coffee (13P), or dark gray (19P and 25P). Tiles made of 7P, 10P, and 13P can be used uncoated, while 19P and 25P require the dark gray color to be masked by glazing.

These cobalt-nickel and tin-lead slags can thus be used in making building ceramics. Although there are considerable differences between the slags in phase and chemical compositions, the parameters in the ceramic tiles are almost identical within these groups.

These slags can replace alkali fluxes, reduce material consumption, reduce reject losses, and increase working lives. The economic effect is 200,000 rubles from the production of one million m^2 of ceramic tiles.

LITERATURE CITED

1. L. P. Chernyak and B. G. Tishchenko, Ceramic Tiles Made from Low-Grade Clays and Industrial Wastes: Survey Information [in Russian], Ser. 5, No. 2, VNIIÉSM (1986).
2. A. A. Shpokauskas, V. M. Vasilyauskas, P. V. Kichas, et al., "The effects of FeO on mullite formation from kaolin," Trudy Instituta NIIteploizolyatsiya, No. 4, 226-236 (1970).
3. A. S. Berezhnoi, Multicomponent Oxide Systems [in Russian], Naukova Dumka, Kiev (1970).
4. A. A. Pashchenko, Silicate Physical Chemistry [in Russian], Izd. MGU, Moscow (1986).
5. I. I. Plyusnina, Silicate Infrared Spectra [in Russian], Izd. MGU, Moscow (1967).
6. Wollastonite [in Russian], Nauka, Moscow (1982).
7. M. Yu. Chop, A. A. Pashchenko, and I. A. Sychevskii, "Dense sintering ceramic tiles made with the addition of silicomanganese slag," Steklo Keram., No. 12, 4-5 (1986).